Inorganica Chimica Acta, *87* (1984) 159–164

Complexes of Tetracyanobiimidazole. 4. Dimers of Cu(I)

P. G. RASMUSSEN*, J. E. ANDERSON

Department of Chemistry, University of Michigan, Ann Arbor, Mich. 48109, U.S.A.

and J. C. BAYÓN*

Department de Química Inorgànica, Facultat de Ciències, Universitat Autònoma de Barcelona, Bellaterra, Barcelona, Spain

Received November 29, 1983

In this paper we describe dimeric complexes of Cu(I) with 4,4′,5,5′-tetracyano-2,2′-biimidazole (H_2-Tcbiim). These compounds contain the dianion (Tcbiim^{2-}) acting as a quadridentate bridge between Cu(I) ions in combinations with phosphine, phosphite, pyridine, and quinuclidine ligands. Syntheses and interconversions among these species are recorded. The structure of $Cu_2[P(OPh)_3]_2(Py)_2$Tcbiim·Py was determined by X-ray crystallography. The composition $Cu_2P_2O_6C_{61}N_{11}H_{45}$ crystallizes in the $P\bar{1}$ triclinic space group with $a = 10.456(3)$ Å, $b = 15.060(5)$ Å, $c = 10.438(2)$ Å, $\alpha = 94.89(2)$, $\beta = 115.93(2)$, $\gamma = 72.76(2)$ and $Z = 1$ molecule per cell. A final agreement of $R = 0.035$, $R_w = 0.042$ was obtained for 2743 observed reflections. The dimeric molecule has an inversion center between the 2,2′ carbon atoms of Tcbiim^{2-}. Each Cu atom is tetrahedrally coordinated with angles ranging from 101°–126°. As a result of steric crowding by the phenyl rings of $P(OPh)_3$ the copper atoms are somewhat sequestered. The influence of the steric and electronic factors can be seen in the oxidation potentials obtained from cyclic voltammetry. The potentials for the successive one electron oxidation of the dimers vary greatly with the donor strength of the ligands.

Introduction

Binuclear copper complexes are of interest for a variety of reasons. They have been the basis for numerous studies of magnetic interactions, multimetal center reactions, and mixed valency [1]. The uses of copper reagents in organic syntheses [2] and the discoveries of the roles of copper in biological systems [3] have added impetus to these investigations. Greater understanding of the biological aspects has in turn led to a reexamination of copper compounds in medicinal chemistry [4]. Progress in these various areas requires increased basic knowledge regarding the redox potentials, geometry, and reactivity of copper species, and is of particular interest for dimeric systems.

We have been directing our efforts toward the challenge of controlling both the geometry and oxidation potential of Cu(I) dimers in an effort to systematically synthesize a mixed valence system. Our approach is to use a pi accepting, aromatic, dianion as the bridging group, and test a variety of other donor types in combination with it. We describe here a series of bridged copper(I) dimers in which the oxidation potentials are substantially altered, while the geometry about the copper atoms remains essentially unchanged.

Recently we reported the properties of a remarkable new ligand 4,4′,5,5′-tetracyano-2,2′-biimidazole (H_2Tcbiim) [5]. We have also reported its use in forming complexes with Rh(I), Ir(I), Mo(0), Pd(II), and Pt(II) [6–8]. In addition a preliminary report on the chemistry of H_2Tcbiim with copper and silver has been published [9].

In this paper we describe the syntheses; cyclic voltammagrams and solid state IR spectra of the series of dimers $Cu_2(PPh_3)_4$Tcbiim, $Cu_2(PPh_3)_2(Py)_2$Tcbiim, $Cu_2[P(OPh)_3]_2$Tcbiim, $Cu_2[P(OPh)_3]_2(Py)_2$Tcbiim and $Cu_2[P(OPh)_3]_2(Q)_2$Tcbiim where PPh_3 is triphenylphosphine, $P(OPh)_3$ is triphenylphosphite, Py is pyridine and Q is quinuclidine. The X-ray crystal structure of $Cu_2[P(OPh)_3]_2(Py)_2$Tcbiim·Py is presented. In addition, ^{13}C and ^{31}P NMR of the compounds $Cu_2(PPh_3)_4$Tcbiim, $Cu_2[P(OPh)_3]_2$Tcbiim and $Cu_2[P(OPh)_3]_2(Py)_2$Tcbiim are discussed.

Experimental

The ligands PPh_3, $P(OPh)_3$ and quinuclidine were purchased from Aldrich Chemical Co., Milwaukee, WI, USA and used without further purification. The compounds H_2Tcbiim, $Cu_2(Py)_2$Tcbiim and $Cu_2(CH_3CN)_4BF_4$ were prepared following published procedures [5, 9]. Infrared spectra were recorded on a Perkin Elmer 1330 spectrophotometer. Fourier Transform NMR were measured on a Bruker WM-

---

*Authors to whom correspondence should be addressed.

0020-1693/84/$3.00

360 spectrometer calibrated with ^{13}C and ^{31}P shifts as positive downfield relative to TMS and H_3PO_4. Cyclic voltammagrams were measured using a model 173 Potentiostat/Galvanostat equipped with a model 176 current to voltage converter made by Princton Applied Research. A Tektronix FG 504 40 MHz function generator was used to generate the triangular potential wave and control the frequency of the potential wave. Since all CV measurements were made in non-aqueous solvents, potentials are reported using ferrocene as a internal reference [10]. Elemental analysis were done by Spang Microanalytical Laboratory, Eagle Harbor, MI or at Galbraith Laboratories, Knoxville, TN, USA. All reactions were carried out in inert atmosphere by Schlenk technique.

Preparation of $Cu_2(PPh_3)_4$Tcbiim

To a methanol solution of $Cu(CH_3CN)_4BF_4$ a slight excess of PPh_3 was added, followed by a stoichiometric amount of H_2Tcbiim. After 15 minutes a white precipitate formed. After three hours of stirring an air stable product was collected by filtration. Yield 90%. *Anal.* Calcd for $Cu_2P_4C_{82}N_8H_{60}$: C, 69.94; N, 7.96; H, 4.26. Found: C, 70.43; N, 7.99; H, 4.36.

Preparation of $Cu_2(PPh_3)_2(Py)_2$Tcbiim

(a) $Cu_2(PPh_3)_4$Tcbiim was dissolved in a minimum amount of pyridine. Hexane was then added to precipitate the product. Yield 72%. *Anal.* Calcd for $Cu_2P_2C_{56}N_{10}H_{40}$: C, 64.57; N, 13.44; H, 3.84. Found: C, 64.38; N, 13.55; H, 3.91.

(b) To a suspension of $Cu_2(Py)_2$Tcbiim in methylene chloride a slight excess of PPh_3 was added. As the reaction proceeded a solution formed and reduction of volume resulted with precipitation. The product was washed with acetone. Yield 55%.

Preparation of $Cu_2[P(OPh)_3]_2$Tcbiim

To a solution of $Cu(CH_3CN)_4BF_4$ in acetone a slight excess of $P(OPh)_3$ was added followed by a stoichiometric amount of H_2Tcbiim which resulted in the immediate precipitation. After stirring for four hours, the air stable product was collected by filtration. Yield 87%. *Anal.* Calcd for $Cu_2P_2O_6C_{46}N_8H_{30}$: C, 56.38; N, 11.44; H, 3.06. Found: C, 56.34; N, 11.48; H, 3.00.

Preparation of $Cu_2[P(OPh)_3]_2(Py)_2$Tcbiim

(a) The compound $Cu_2[P(OPh)_3]_2$Tcbiim was dissolved in a minimum amount of pyridine. Hexane was added to force precipitation of a white solid which from analysis contains a solvated pyridine. Yield 50%. *Anal.* Calcd for $Cu_2P_2O_6C_{62}N_{11}H_{45}$: C, 60.20; N, 12.66; H, 3.70. Found: C, 60.02; N, 12.31; H, 3.74.

(b) To a suspension of $Cu_2(Py)_2$Tcbiim in methylene chloride a slight excess of $P(OPh)_3$ was added. After twelve hours of stirring the product was collected. Yield 56%.

Preparation of $Cu_2[P(OPh)_3]_2(Q)_2$Tcbiim

To a suspension of $Cu_2[P(OPh)_3]_2$Tcbiim in THF a slight excess of quinuclidine was added, after stirring for six hours all of the reactant was in solution. Upon reducing the volume of solvent and layering with hexane the white product formed. Yield 20%. *Anal.* Calcd for $Cu_2P_2O_6C_{60}N_{10}H_{56}$: C, 59.92; N, 11.65; H, 4.66. Found: C, 58.91; N, 11.31; H, 4.86.

Collection of X-Ray Data and Solution of Structure

Single crystals of $Cu_2[P(OPh)_3]_2(Py)_2$Tcbiim·Py were grown by layering a pyridine solution of the compound with hexane. After 36 hours at 4 °C large, clear hexagon crystals had formed. An individual crystal was cut and sealed in a 0.3 mm capillary for data collection on a Syntex P$\bar{1}$ four circle diffractometer.

Axial X-ray photographs of the crystal did not show any apparent symmetry, indicating triclinic space group. The structure refined successfully in the $P\bar{1}$ space group. The standard reflection intensities varied by less than 2 per cent during the collection of the data. The structure was solved by conventional heavy atom and difference Fourier methods. The pyridine of crystallization was treated as a six membered carbon ring since it was located about an inversion point of the cell. After refining to anisotropic convergence, [$R = 0.048$, $Rw = 0.042$] hydrogen atom positions were calculated along with their thermal parameters. The contribution of the hydrogen atoms to the data was then calculated based on their calculated positions and thermal parameters and subtracted from the data. Further anisotropic refinement led to final convergence. [$R = 0.035$, $Rw = 0.042$]. No absorption correction was necessary since the maximum and minimum transmission factors differed by only 8%. The final difference map showed no peak greater than 0.35 e/Å^3. The crystal data are summarized in Table I, the atomic coordinates in Table II, and the programs used are cited in reference [11].

TABLE I. Crystallographic Parameters for $Cu_2[P(OPh)_3]_2(Py)_2$Tcbiim·Py.

Space group	$P\bar{1}$
a Å	10.456(3)
b Å	15.060(5)
c Å	10.438(2)
alpha (deg.)	94.89(2)
beta	115.93(2)

(continued on facing page)

TABLE I *(continued)*

gamma	72.76(2)
Volume Å^3	1410.0(7)
Molecular wt	1216.0
Z	1
d obs	1.30 g/cm
d calc	1.34 g/cm
Crystal dimensions	0.16 × 0.25 mm
Crystal shape	hexagon
Radiation	λ(MoKα) 0.71069
Linear abs coeff	8.715 cm^{-1}
Transmission factor	0.87–0.80
Scan speed	2.5–12
Ratio of bkd/peak scan	0.8
Standard reflections	(2, 2, 0) (1, 4, 0) (1, 1, −3)
Dev. of stds.	<2%
Two theta limit	45
Reflections collected	3953
Refl. with $F' \geqslant 3\sigma(F^2)$	2743

TABLE II. Atomic Coordinates.

Atom	X	Y	Z
Cu	0.27353(4)	0.16617(2)	0.44335(3)
P	0.19349(8)	0.25096(5)	0.58420(7)
O(1)	0.30589(21)	0.24345(13)	0.75047(18)
O(2)	0.05496(21)	0.24093(14)	0.60566(19)
O(3)	0.14424(24)	0.36158(13)	0.55902(21)
C(11)	0.42128(32)	0.16014(20)	0.80721(26)
C(12)	0.39123(32)	0.07600(22)	0.78843(29)
C(13)	0.50875(38)	−0.00403(22)	0.83243(33)
C(14)	0.65228(38)	0.00071(24)	0.91690(33)
C(15)	0.67828(34)	0.08559(27)	0.93679(32)
C(16)	0.56316(35)	0.16676(22)	0.88229(30)
C(21)	−0.07899(33)	0.24775(23)	0.48392(31)
C(22)	−0.09928(37)	0.16699(24)	0.41548(35)
C(23)	−0.23321(47)	0.17311(33)	0.29666(43)
C(24)	−0.34101(42)	0.25525(41)	0.24939(41)
C(25)	−0.31892(42)	0.33490(32)	0.31914(47)
C(26)	−0.18543(38)	0.33229(24)	0.43996(38)
C(31)	0.16336(35)	0.40335(18)	0.45615(31)
C(32)	0.30083(38)	0.40972(25)	0.48288(39)
C(33)	0.31422(49)	0.45393(32)	0.38134(60)
C(34)	0.19469(71)	0.49198(29)	0.25763(57)
C(35)	0.05777(53)	0.48544(27)	0.23376(42)
C(36)	0.04129(36)	0.44094(23)	0.33313(37)
N(6)	0.18937(25)	0.21127(14)	0.23612(22)
C(61)	0.05399(38)	0.20872(25)	0.14713(31)
C(62)	0.01425(43)	0.23618(30)	−0.00137(36)
C(63)	0.06585(51)	0.26533(27)	−0.05383(38)
C(64)	0.21105(44)	0.26770(25)	0.04312(38)
C(65)	0.26486(33)	0.24090(20)	0.18356(30)
N(1)	0.30036(22)	0.01702(14)	0.42017(20)
C(1)	0.55295(26)	0.02585(17)	0.52667(24)
N(2)	0.51218(22)	0.11848(14)	0.52772(20)
C(2)	0.64532(27)	0.13846(17)	0.59142(26)
C(3)	0.24130(27)	−0.05538(18)	0.37756(25)
C(4)	0.65871(28)	0.22967(21)	0.62802(27)
N(4)	0.67221(28)	0.30106(18)	0.66496(28)
C(5)	0.08564(33)	−0.04499(19)	0.30604(30)
N(5)	−0.03751(30)	−0.04019(19)	0.24908(32)
C(71)	0.55125(69)	0.44141(29)	−0.07897(48)
C(72)	0.36358(45)	0.50856(36)	−0.00979(53)
C(73)	0.41639(67)	0.44981(33)	−0.08738(44)

Discussion

An ORTEP view of $Cu_2[P(OPh)_3]_2(Py)_2$Tcbiim is shown in Fig. 1. Bond distances and angles are provided in Tables III and IV. In addition to the inversion center which bisects the 2,2′ carbon-carbon bond, the bond lengths show that Tcbiim^{2-} is acting as a symmetrically bridging quadridentate ligand. The geometry about the copper atom is distorted tetrahedral, as is evident from the angles and the dihedral angle between the two planes N(1)–Cu–N(2) and P–Cu–N(6) of 101.5°. The Tcbiim^{2-} ion and the Cu atom are coplanar, with the largest deviation from an idealized plane of these atoms is 0.05 Å. The metal–metal distance across the ligand is 5.37 Å compared to 5.46 Å in the case of Rh(I), and 5.96 Å in a Mo(0) dimer [12, 7].

The Cu to P bond distance is 2.15 Å and the Cu to pyridine nitrogen distance is 2.04 Å, somewhat shorter than the Tcbiim^{2-} nitrogen bonding distances of 2.18 Å and 2.15 Å. These distances are well within the normal Cu(I) to phosphite and nitrogen bond distances [13, 14, 15]. The positioning of the phosphite phenyl rings is intriguing. Along with the pyridine ring, they appear to form a shell around the copper atom.

The IR spectra, especially in the nitrile region, for the related compounds suggest that they all have similar structures. In all cases, except for the phosphite dimer, the CN band is a sharp singlet occurring in the range of 2220 cm^{-1}. This suggests equivalent nitriles and a structure in which Tcbiim^{2-} acts as symmetrical a quadridentate bridging ligand. In the case of the phosphite dimer, the CN band is split. We are not sure of the structure in the solid state, but the ^{13}C NMR (in DMSO) shows that the solvent coordinates with the compound. This is clearly seen in the DMSO signal, and the six Tcbiim^{2-} signals at 149.8, 148.4; 118.5, 117.5; 112.3, 111.9 ppm relative to TMS. These splittings indicate a mirror plane along the C–C bond connecting the two imidazole rings. The ^{31}P NMR gives only one sharp signal. It appears the DMSO fills the fourth coordination site and that Tcbiim^{2-} is acting as a quadridentate bridging ligand. The NMR spectra of $Cu_2(PPh_3)_4$Tcbiim show that this compound is

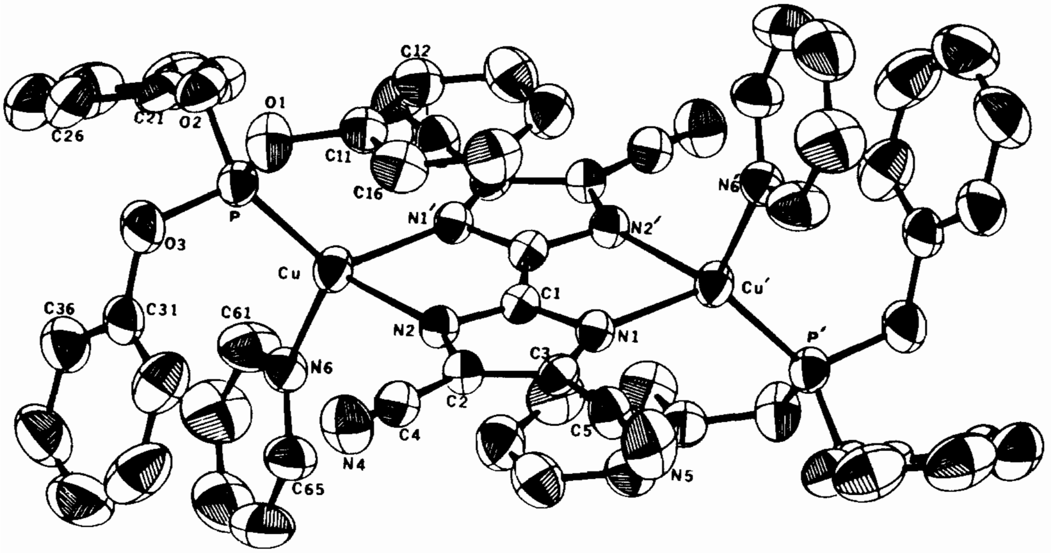

Fig. 1. ORTEP view of $Cu_2[P(OPh)_3]_2(Py)_2$Tcbiim.

TABLE III. Selected Interatomic Distances $Cu_2[P(OPh)_3]_2(Py)_2$Tcbiim·Py.

(A) *Distances from central copper atom*	
Cu–P	2.148(1)
Cu–N(6)	2.036(2)
Cu–N(1)	2.185(2)
Cu–N(2)	2.154(2)
Cu–Cu	5.37
(B) Distances within Tcbiim	
C(1)–N(1)	1.344(3)
C(1)–N(2)	1.333(2)
N(1)–C(3)	1.358(3)
C(3)–C(5)	1.427(4)
C(3)–C(2)	1.389(3)
C(5)–N(5)	1.140(3)
C(2)–C(4)	1.425(4)
C(4)–N(4)	1.138(3)
C(2)–N(2)	1.428(5)
C(1)–C(1)'	1.428(5)
(C) Distances within $POPh_3$	
P–O(1)	1.605(2)
P–O(2)	1.602(2)
P–O(3)	1.599(2)
O(1)–C(11)	1.409(3)
O(2)–C(21)	1.403(3)
O(3)–C(31)	1.402(3)
(D) Distances within Py	
N(6)–C(61)	1.321(4)
N(6)–C(65)	1.324(3)
C(61)–C(62)	1.432(4)
C(62)–C(63)	1.362(5)
C(63)–C(64)	1.419(5)
C(64)–C(65)	1.369(4)

TABLE IV. Selected Interatomic Angles and Planes $Cu_2[P(OPh)_3]_2(Py)_2$Tcbiim·Py.

(A) Angles about central copper atom	
N(6)–Cu–P	119.49(7)
N(6)–Cu–N(2)	108.38(9)
P–Cu–N(2)	100.81(8)
P–Cu–N(1)	113.91(6)
N(2)–Cu–N(1)	125.96(6)
(B) Angles within Tcbiim	
C(1)–N(1)–C(3)	102.41(20)
N(2)–C(1)–N(1)	116.59(20)
N(2)–C(1)–C(1)'	122.09(28)
N(1)–C(1)–C(1)'	121.33(28)
C(1)–N(2)–C(2)	102.95(20)
N(2)–C(2)–C(3)	108.37(22)
N(2)–C(2)–C(4)	123.63(23)
C(3)–C(2)–C(4)	127.80(24)
N(1)–C(3)–C(2)	109.66(22)
N(1)–C(3)–C(5)	123.95(23)
C(2)–C(3)–C(5)	126.34(24)
N(4)–C(4)–C(2)	176.21(31)
N(5)–C(5)–C(3)	177.47(39)
(C) Angles within triphenylphosphite	
O(3)–P–O(1)	98.41(11)
O(3)–P–O(2)	99.12(11)
O(1)–P–O(2)	96.48(11)
C(11)–O(1)–P	118.57(16)
C(21)–O(2)–P	118.04(16)
C(31)–O(3)–P	121.68(16)
Distance from best plane of Cu and Tcbiim	
Atom	Perp. dist to plane
N(1)	0.046

(continued on facing page)

TABLE IV *(continued)*

Distance from best plane of Cu and Tcbiim

Atom	Perp. dist to plane
C(1)	0.011
N(2)	−0.076
C(2)	−0.064
C(3)	0.084
C(4)	−0.023
N(4)	0.079
C(5)	0.001
N(5)	−0.059
Cu	−0.045

symmetrically bridged. In the ^{13}C NMR there are three signals for Tcbiim^{2-} at 151.2, 119.6, and 113.4 ppm relative to TMS, requiring an inversion point between the two imidazole rings and ^{31}P NMR gives only one signal showing equivalent phosphines. The NMR of $Cu_2[P(OPh)_3]_2(Py)_2$Tcbiim in DMSO shows only one ^{13}C signal for Tcbiim^{2-} and only one ^{31}P signal. There was no indication of DMSO coordinating with Cu in this compound.

The CV measurements were all completed in deoxygenated, freshly distilled solvents. In the case of $Cu_2(PPh_3)_4$Tcbiim, $Cu_2[P(OPh)_3]_2(Q)_2$Tcbiim and $Cu_2(PPh_3)_2(Py)_2$Tcbiim the solvent was CH_2Cl_2 while for $Cu_2[P(OPh)_3]_2$Tcbiim and $Cu_2[P(OPh)_3]_2(Py)_2$Tcbiim the solvent was DMSO. The use of DMSO as a solvent was necessary to achieve a reasonable concentration. The supporting electrolyte in all cases was $N(C_4H_9)_4PF_6$. The concentration of the supporting electrolyte was 0.1 *M* and of the electroactive compounds was typically 0.005 *M*. The reference electrode was $Ag/AgNO_3$ in acetonitrile, but all potentials were calibrated relative to an internal ferrocene/ferricinium couple (0.400 V *vs.* NEH).

The shape of the cyclic voltammagrams of the five copper(I) dimers indicate that their oxidation is irreversible. Only in the case of $Cu_2[P(OPh)_3]_2(Q)_2$Tcbiim did the CV approach a reversible pattern, and there appeared to be two distinct oxidation–reduction waves. For $Cu_2(PPh_3)_2(Py)_2$Tcbiim, the second wave overlaps with ferrocene, so a good measurement was not possible in this case. The potentials *vs.* NHE are summarized in Table V.

The oxidation potentials for the compounds show a definite pattern. When triphenylphosphine is present the oxidation potentials are relatively large. When triphenylphosphite is substituted the potentials are decreased. This pattern is expected since triphenylphosphine is known to stabilize copper(I) more than triphenylphosphite. The addition of pyridine in either case caused the oxidation potential to be slightly reduced. The addition of quinuclidine to the copper phosphite framework caused only a small change in the oxidation waves, but a large change in the reduction waves.

TABLE V. Oxidation and Reduction Potentials (*vs.* NHE).

Compound	Oxidation	Reduction
$Cu_2(PPh_3)_4$Tcbiim	1.28 V	−0.96
	1.85 V	−0.61
$Cu_2(PPh_3)_2(Py)_2$Tcbiim	0.40 V	−0.77 V
	1.64 V	−0.07 V
$Cu_2[P(OPh)_3]_2$Tcbiim xDMSO	0.29 V	−1.20 V
	0.76 V	−0.32 V
$Cu_2[P(OPh)_3]_2(Py)_2$Tcbiim	0.27 V	−0.92 V
	0.48 V	−0.32 V
$Cu_2[P(OPh)_3]_2(Q)_2$Tcbiim	0.27 V	0.07 V
	1.06 V	0.79 V

Conclusion

Several interesting features of copper chemistry have emerged from this investigation. First, we observe that Cu(I) has a strong affinity for Tcbiim^{2-} and is especially prone to forming dimers with it. These dimers, once formed, are sufficiently robust to allow a variety of substitution reactions on this core. Some of the interconversions which we have examined are summarized in Fig. 2. This is clearly a fruitful area for further work, and we are currently looking into reactions with other ligands of low electronegativity for which copper has traditionally been a difficult case. Second, we note that redox potentials are variable over a wide range as a function of substituent. Also, as the ligand system becomes more sterically protective, the cyclic voltammagrams appear to become more reversible. We believe this indicates that it will be possible with the right combination of donors and stereochemistry to stabilize a mixed-valence system in which minimal coordination sphere rearrangement occurs under one electron oxidation. In that case the interaction between the metal centers would be predicted to be large. Our investigations towards such a system are continuing. Finally, our crystallographic results confirm that Cu(I) is tetrahedrally coordinated, even when several moderately strong pi acceptors are present. This

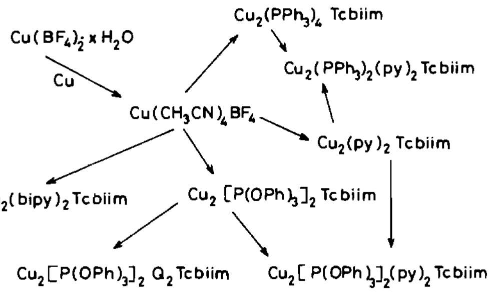

Fig. 2. Interconversions.

casts some doubt on the lower coordination numbers which are sometimes postulated and suggests that further scrutiny of this feature is desirable.

Acknowledgment

J.C.B. wishes to thank the Fulbright Commission and the U.S.A.-Spain Joint Committee for post-doctoral support. J.E.A. is grateful for support as a Ruthruff Fellow of the chemistry department of U. of M.

Supplementary Information

Tables of structure factors, anisotropic thermal parameters, calculated hydrogen positions, and least squares planes are available upon request to either of the senior authors.

References

1 L. Casella and S. Ghelli, *Inorg. Chem., 22*, 2458 (1983). (This paper contains an unusually complete list of citations for being a non-review type article.)

2 G. H. Posner, 'An Introduction to Synthesis Using Organocopper Reagents', Wiley/Interscience, New York 1980.

3 S. K. Mandel and K. Nag, *Inorg. Chem., 22*, 2567 (1983).

4 J. R. J. Sorenson, 'Inflammatory Diseases and Copper', Humana Press, Crescent Manor, P.O. Box 2148, Clifton NJ U.S.A. 07015.

5 P. G. Rasmussen, R. L. Hough, J. E. Anderson, O. H. Bailey and J. C. Bayón, *J. Am. Chem. Soc., 104*, 6155 (1982).

6 P. G. Rasmussen, O. H. Bailey, J. C. Bayón and W. M. Butler, *Inorg. Chem.*, in press.
P. G. Rasmussen, O. H. Bailey and J. C. Bayón, *Inorg. Chem., 23*, 338 (1984).

7 P. G. Rasmussen and J. C. Bayón, *Inorg. Chem., 23*, 343 (1984).

8 P. G. Rasmussen, O. H. Bailey and J. C. Bayón, *Inorg. Chim. Acta, 86*, 107 (1984).

9 P. G. Rasmussen and J. A. Anderson, *Polyhedron, 2*, 547 (1983).

10 R. R. Gagne, C. A. Koval and G. C. Lisensky, *Inorg. Chem., 19*, 2855 (1980).

11 Computer programs used during the structural analysis were SYNCOR (data reduction by W. Shmonsees), N. W. Alcock's absorption program, FORDAP (Fourier synthesis by A. Zalkin), ORFLS (full matrix least-squares refinement by Busing, Martin and Levy), ORFFE (distances, angles, and their esd's by Busing, Martin, and Levy), ORTEP (thermal ellipsoid drawings by C. K. Johnson), HATOMS (hydrogen atom positions by A. Zalkin), PLANES (least-squares by D. M. Blow), and PLUTO (crystallographic plotting program supplied by University Chemical Laboratory, Cambridge, England). Atomic scattering factors were obtained from D. T. Cromer and J. T. Waber.

12 S. W. Kaiser, R. B. Saillant, W. M. Butler and P. G. Rasmussen, *Inorg. Chem., 15*, 2681 (1976).

13 R. F. Ziolo, A. P. Gaughan, Z. Dori, C. G. Pierpont and R. Eisenberg, *Inorg. Chem., 10*, 1289 (1971).
F. A. Cotton and J. Takats, *J. Am. Chem. Soc., 92*, 2353 (1970).

14 G. C. Messmer and G. J. Palenik, *Can. J. Chem., 47*, 1440 (1969).

15 V. G. Albano, P. L. Bellon, G. Ciani and M. Marassero, *J. Chem. Soc. Dalton Trans.*, 171 (1972).